Supplementary Information for “Robust Simulations of Many-Body Symmetry-Protected Topological Phase Transitions on a Quantum Processor”

Ruizhe Shen,[1,*] Tianqi Chen,[1,2,†] Bo Yang,[2] Yin Zhong,[3,4,‡] and Ching Hua Lee[1,§]

[1] *Department of Physics, National University of Singapore, Singapore 117551*

[2] *School of Physical and Mathematical Sciences, Nanyang Technological University, Singapore 639798, Singapore*

[3] *Key Laboratory of Quantum Theory and Applications of MoE and School of Physical Science and Technology, Lanzhou University, Lanzhou 730000, People's Republic of China*

[4] *Lanzhou Center for Theoretical Physics, Key Laboratory of Theoretical Physics of Gansu Province, Lanzhou University, Lanzhou 730000, People's Republic of China*

(Dated: September 16, 2025)

Supplementary note 1 IBM Q Quantum hardware

We present data from the “ibm-brisbane” device, which has a total of 127 qubits. For simulations in this work, we utilize the qubit chain $[10, 9, 8, 7, 6, 5, 4, 3, 2, 1, 0]$ chosen for its optimal noise levels. The readout error rate of ancilla qubits 9 and 10 is approximately 0.6%. This low error rate ensures robust simulations, which require ancilla post-selection.

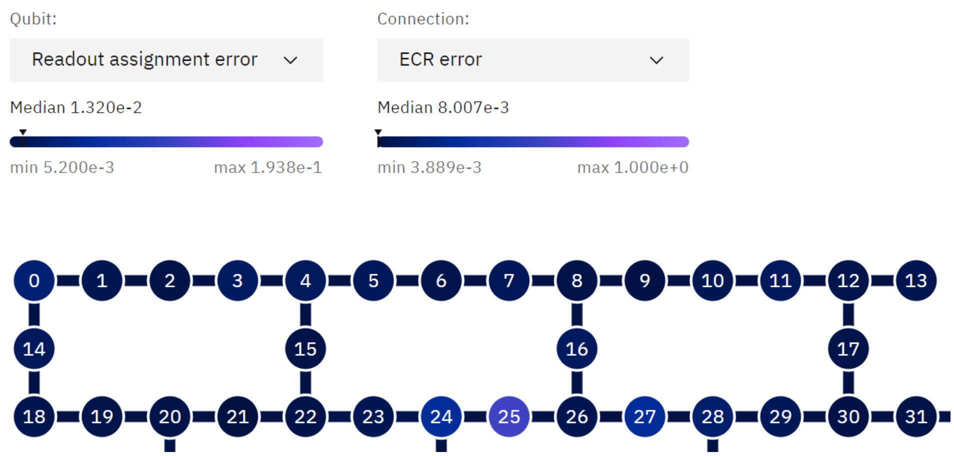

Supplemental Figure 1. Noise data of the ”ibm-brisbane” device. The order of the selected qubit chain is $[10, 9, 8, 7, 6, 5, 4, 3, 2, 1, 0]$. The average ECR gate error rate for the selected connections is approximately 0.5%. Additionally, for the ancilla qubits 9 and 10, the readout error rate is 0.6%.

Supplementary note 2 error mitigation

In our work, we employ the method of zero-noise extrapolation (ZNE) to mitigate noise effects. This technique involves amplifying noise levels in quantum simulations and then using these data points to extrapolate back to a theoretical zero-noise limit.

We introduce a more scalable framework based on variational circuits, as illustrated in FIG.2. The initial blue block represents the original trained circuit. Subsequently, additional green identity blocks are introduced to amplify noise effects and simulate conditions for increased error.

In FIG. 3, we present a representative case that demonstrates the implementation of the ZNE method to achieve the results shown in FIG. 4 of the main text. This process involves performing noisy simulations across different circuit layers, including both original and identity layers. Since the structures of all layers are identical, the number of layers serves as an appropriate noise amplification factor. These results of different layers are indicated by the blue dots in FIG. 3). Following this, the zero-noise results are extrapolated from these noisy data points by fitting them

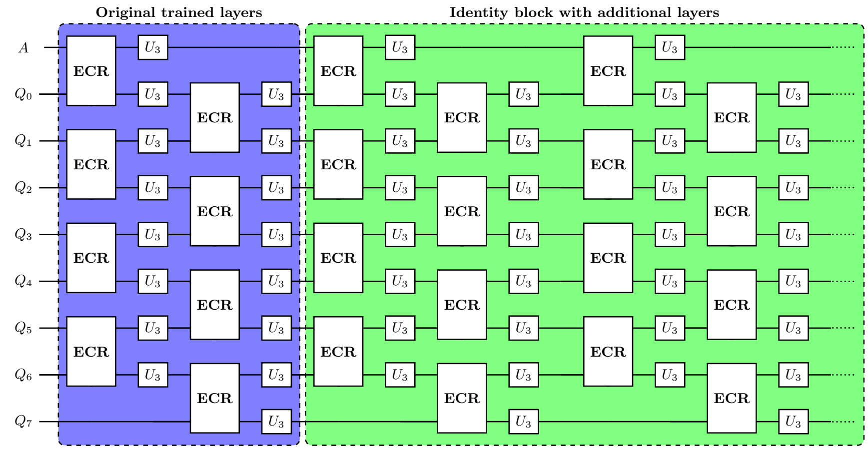

Supplemental Figure 2. Circuit for implementing the method of zero-noise extrapolation (ZNE). The blue block represents the trained circuit used for conducting physical simulations of the quantum imaginary-time evolution or other processes. The green block, consisting of additional layers, serves as an identity function to amplify the impact of gate errors.

to the red curves and extending the fit to the zero-layer limit. These results illustrate how the ZNE method mitigates noise, enabling our simulations to approach theoretical zero-noise conditions.

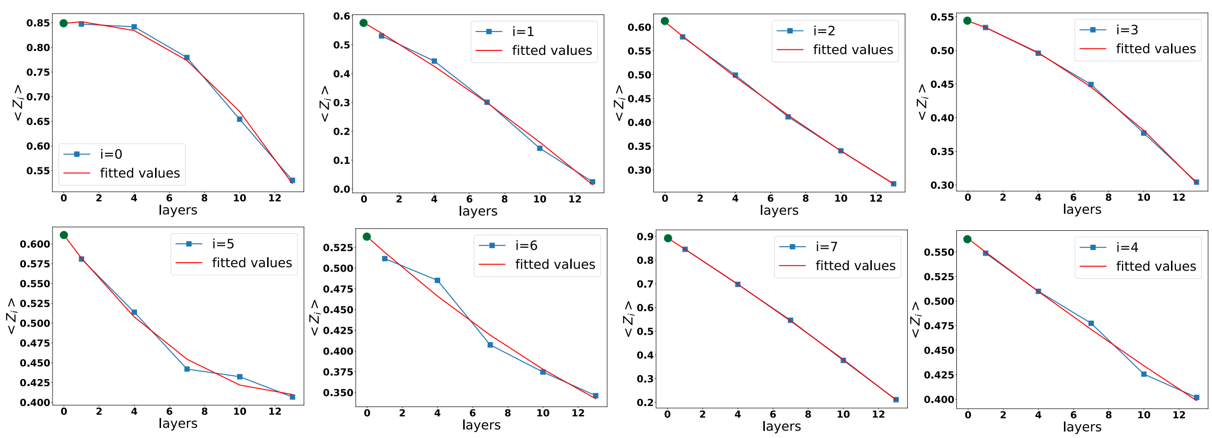

Supplemental Figure 3. Illustration of the implementation of the zero-noise extrapolation method. These data on the magnetizations on sites labeled by different positions i correspond to the results shown in FIG. 4 of the main text. The entire circuit consists of trained layers combined with identity layers. The zero-noise results (green dots) are obtained by extrapolating the noisy data, represented by the blue dots, to the zero-layer point using the fitted red curves.

Supplementary note 3 sampling errors in simulators

As discussed in the main text, we demonstrate that significant sampling errors emerge in the measurement of a density matrix on quantum computers. To understand these errors further, we examine the impact of the number of measurement shots, as shown in FIG. 4. The entanglement gap becomes evident as the number of shots increases. However, a substantial increase in the number of shots from 5000 to 200000 does not yield significant improvements, highlighting the inevitability of sampling errors on current quantum processors.

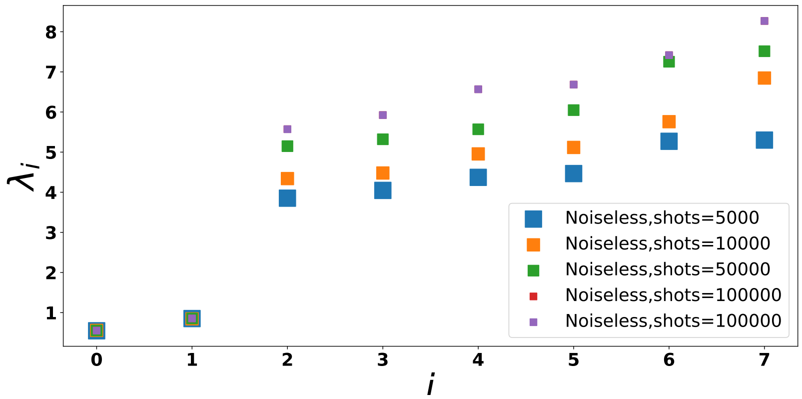

Supplemental Figure 4. Estimation of the sampling error in quantum state tomography. We classically measure the entanglement spectrum of the 3-qubit subspace within a 4-qubit system using noiseless circuits. The reduced density matrix is constructed using the method described by Eq.18 (main text). The squares represent results simulated on the Qiskit noiseless simulator, which includes sampling noise. Notably, increasing the number of measurement shots does not lead to significant improvement. Other parameters are $g = 2.5$ and $J = h = 1$.

Supplementary note 4 additonal simulation results

Here, we provide additional simulation results. As discussed above, a finite number of circuit shots can introduce statistical errors in the measurement of entanglement gaps. To mitigate this effect, we focus on a stronger SPT phase realized in the regime $g \gg J, h$. The corresponding results are shown in FIG. 5. For noisy simulations on the local simulator, we set the ECR gate error rate as 0.5%, and the readout error rate as 0.6%. In this strong SPT regime, FIG.5(a) shows that the lowest-lying states (0–3) remain in good agreement across all methods, while deviations in higher states can be quantified as $\delta\epsilon \approx 10^{-5} - 10^{-40}$, with ϵ denoting the eigenvalue of the reduced density matrix. The resulting entanglement spectrum in FIG.5(b) reveals a robust entanglement gap separating the lowest two levels from the rest. A direct comparison of the raw eigenvalues ϵ is shown in FIG.5(c), where all data sets agree within numerical precision. Importantly, these results demonstrate that the apparent discrepancies in FIG. 5(a) are visually amplified by the logarithmic operation, and do not affect the identification of the entanglement gap.

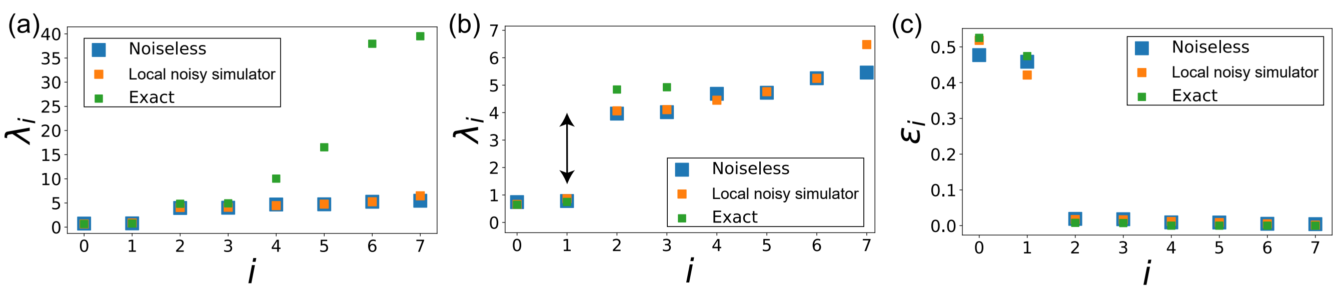

Supplemental Figure 5. Additional simulations of entanglement gaps in a strong SPT phase. We measure the entanglement spectrum of the 3-qubit subspace within a 4-qubit system.Here, ϵ_i denotes the i-th eigenvalue of the reduced density matrix, and $\lambda_i = -\ln(\epsilon_i)$ gives the corresponding entanglement spectrum. (a) shows the full entanglement spectrum: the first four states agree well across all methods, while discrepancies emerge in the higher states. (b) focuses on the range $\lambda_i < 7$, revealing a clear entanglement gap separating the lowest two states from the rest. (c) presents the raw eigenvalues ϵ_i, where nearly all states display good agreement; the deviations shown in (a) are visually amplified by the logarithmic operation. Other parameters are $g = 5$ and $J = h = 0.2$. For all results, we set the number of runs as 50000.

* e0554228@u.nus.edu

† tqchen@nus.edu.sg
‡ zhongy@lzu.edu.cn
§ phylch@nus.edu.sg